KI REPORTS
KIReports.org



# Multiple Myeloma–Associated Ig Light Chain Crystalline Cast Nephropathy



Hirotoshi Matsumura[1], Yusuke Furukawa[1], Takashi Nakagaki[1], Chikako Furutani[1], Sayaka Osanai[1], Keiichi Noguchi[2], Masafumi Odaka[1], Masafumi Yohda[3], Hiroshi Ohtani[4], Yoshihiro Michishita[5], Yoshinari Kawabata[5], Atsushi Kitabayashi[5], Sho Ikeda[6], Mizuho Nara[6], Atsushi Komatsuda[6], Naoto Takahashi[6] and Hideki Wakui[1]

[1]Department of Life Science, Graduate School of Engineering Science, Akita University, Akita, Japan; [2]Instrumentation Analysis Center, Tokyo University of Agriculture and Technology, Tokyo, Japan; [3]Department of Biotechnology and Life Science, Graduate School of Engineering, Tokyo University of Agriculture and Technology, Tokyo, Japan; [4]Department of Nephrology, Akita Kousei Medical Center, Akita, Japan; [5]Department of Hematology, Akita Kousei Medical Center, Akita, Japan; and [6]Department of Hematology, Nephrology, and Rheumatology, Graduate School of Medicine, Akita University, Akita, Japan

**Correspondence**: Hideki Wakui, Department of Life Science, Graduate School of Engineering Science, Akita University, 1-1 Tegatagakuen-machi, Akita City, Akita 010-8502, Japan. E-mail: wakui517@gipc.akita-u.ac.jp

**Received 22 April 2020; revised 10 June 2020; accepted 23 June 2020; published online 3 July 2020**

*Kidney Int Rep* (2020) **5,** 1595–1602; https://doi.org/10.1016/j.ekir.2020.06.026


## INTRODUCTION

Renal involvement is a common complication in multiple myeloma (MM), a malignant neoplasm arising from an abnormal proliferation of clonal plasma cells in the bone marrow.[1] MM-associated renal disorders such as amyloidosis and cast nephropathy usually result from the extracellular deposition of monoclonal Ig free light chains (FLCs). Monoclonal Ig FLCs excreted in the urine are referred to as Bence–Jones proteins (BJPs).[2]

Ig light chains (LCs) are classified as either κ LC or λ LC and consist of variable ($V_L$) and constant ($C_L$) domains connected by a joining ($J_L$) segment. The $V_L$ domain contains 3 hypervariable segments termed complementarity-determining regions (CDRs) that are further divided into CDR1, CDR2, and CDR3. Each FLC has unique nephrotoxicity that is related to the amino acid composition of ≥1 of the CDRs.[2] The 2 mature Ig LCs normally complex with 2 heavy chains to form a heterotetramer, whereas BJPs are generally secreted as folded monomers or homodimers that involve the same interfaces as the LC–heavy chain domains of the mature Igs.[3]

Cast nephropathy is the dominant tubulointerstitial lesion associated with patients with MM with acute kidney injury (AKI).[4] The myeloma casts form through binding of the CDR3 region of BJPs to a specific site on Tamm–Horsfall glycoprotein (THP), also known as uromodulin, which is produced by tubular epithelial cells in the distal loop of Henle, and then the cast formation occurs in the distal nephron.[2] The myeloma casts usually exhibit a fractured and brittle appearance with a surrounding cell inflammatory reaction,[1] causing AKI and progressive renal failure. On the other hand, Ig LC crystalline cast nephropathy has been rarely reported in patients with MM with AKI. To the best of our knowledge, there have only been 9 reported cases of MM-associated Ig LC crystalline cast nephropathy since 2000, in which clinical information is available.[S1–S8] Although the primary structure of the disease-causing BJP was clarified in 1 case,[S3] 3-dimensional structural analysis of this BJP by X-ray crystallography was not available in this case. Here, we present the case of MM-associated Ig λ LC crystalline cast nephropathy and describe the primary and 3-dimensional structures of the disease-causing BJP-λ. We also review the clinicopathologic characteristics of this unique nephropathy.

## CASE PRESENTATION

### Clinical History and Initial Laboratory Data

A 73-year-old Japanese woman (initials AK) presented with fatigue and AKI. On admission, her blood pressure was 166/84 mm Hg. A physical examination showed no edema on the extremities. No abnormal signs were observed in the lungs, heart, or abdomen.

Urinalysis showed heavy proteinuria (9.1 g/g creatinine) without hematuria. Glycosuria was not

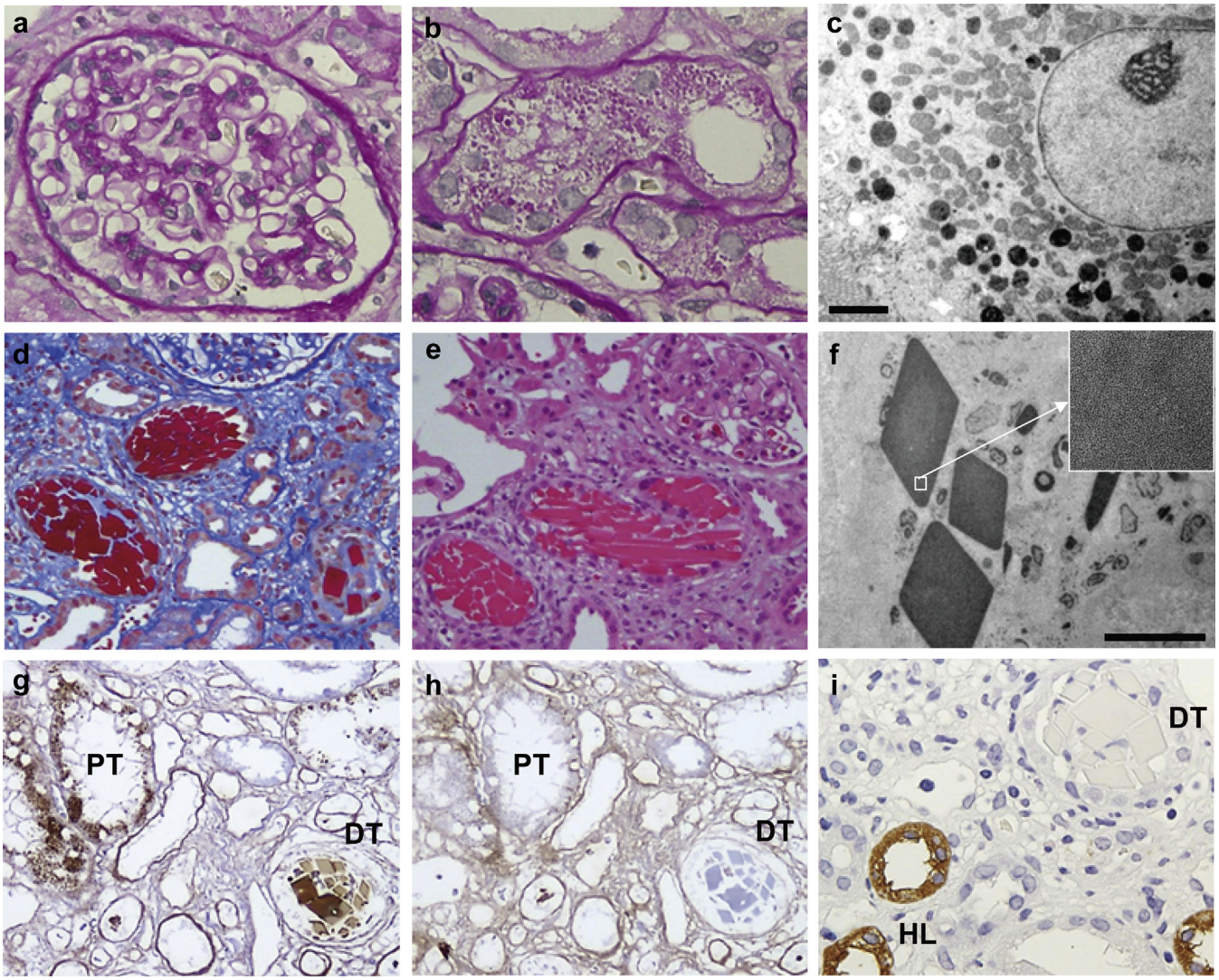


**Figure 1.** Kidney biopsy findings. (a) In the functioning glomeruli, mild mesangial proliferation and epithelial cell swelling were seen on light microscopy (periodic acid–Schiff staining, original magnification ×400). (b) In the proximal tubular epithelial cells, vacuolization and protein reabsorption granules were seen on light microscopy (periodic acid–Schiff staining, original magnification ×400). (c) In the proximal tubular epithelial cells, electron-dense deposits or crystals were not observed on electron microscopy (uranyl acetate and lead citrate staining, original magnification ×3000). Bar = 2 μm. (d) In the distal tubular lumens, casts containing numerous rod-shaped or rhomboid crystals were seen. These casts were fuschinophilic on Masson's trichrome stain (original magnification ×200). (e) Casts in the distal tubular lumens were eosinophilic on hematoxylin and eosin staining (original magnification ×200). (f) Substructural organization was not observed in crystals on electron microscopy (uranyl acetate and lead citrate staining, original magnification ×12,000). Bar = 2 μm. (g) Crystals in the distal tubular lumens (DT) and reabsorption granules in the proximal tubular epithelial cells (PTs) were stained with an anti-λ light chain antibody (original magnification ×200). (h) Crystals in the DT and reabsorption granules in the PT were not stained with an anti-κ light chain antibody (original magnification ×200). (i) An anti-THP antibody stained epithelial cells in the Henle's loops (HL) but not crystals in the DT (original magnification ×400).

found. Urinary $\beta_2$-microglobulin was 48,989 μg/dl. Her leukocyte count, hemoglobin level, and platelet count were 3900/μl, 5.0 g/dl, and 178,000/μl, respectively. Serum total protein was 5.3 g/dl, albumin 3.2 g/dl, blood urea nitrogen 38.3 mg/dl, creatinine 5.59 mg/dl, sodium 146 mEq/l, potassium 3.7 mEq/l, chloride 108 mEq/l, calcium 8.4 mg/dl, ionized phosphate 4.7 mg/dl, IgG 366 mg/dl, IgA <20 mg/dl, and IgM 15 mg/dl. Serum levels of free κ LC and λ LC were 12.6 mg/l and 7910 mg/l, respectively. Immunoelectrophoresis showed monoclonal λ LC in her serum and urine. A bone marrow aspiration revealed an increased number of abnormal plasma cells (52.8%) without intracellular crystal formation (Supplementary Figure S1). Flow cytometry analysis showed an increased number of λ LC–positive cells (85.3%). She was diagnosed with BJP-λ type MM (hereafter designated as BJP-λ AK), and a kidney biopsy specimen was obtained to evaluate her renal disease.

## Kidney Biopsy Findings

On light microscopy, global sclerosis was shown in 5 of 14 glomeruli. The functioning glomeruli showed mild mesangial proliferation and epithelial cell swelling (Figure 1a). There was moderate to severe interstitial fibrosis and tubular atrophy with moderate arteriolar hyalinosis. The proximal tubular epithelial cells had intracellular vacuoles and protein reabsorption granules (Figure 1b). On electron microscopy, neither electron-dense deposits nor crystals were observed in the proximal tubules and the glomeruli (Figure 1c; Supplementary Figure S2A).

Light microscopy revealed that the distal tubular lumens were frequently occupied by numerous crystalline casts with both rod-shaped and rhomboid configurations. The crystalline casts were fuschinophilic on Masson's trichrome staining (Figure 1d) and eosinophilic on hematoxylin and eosin staining (Figure 1e) but were pale on periodic acid–Schiff staining (Supplementary Figure S2B) and negative for amyloid staining. On electron microscopy, the crystalline casts did not exhibit substructural organization (Figure 1f).

Immunofluorescence and immunohistochemical studies were performed in accordance with the procedures described in the Supplementary Methods. The results showed no glomerular staining for IgG, IgA, IgM, κ LC, λ LC, C3, or C1q. The crystalline casts in the distal tubular lumens and the reabsorption granules in the proximal tubules were stained with antihuman λ LC antibody (Figure 1g), whereas these were not stained with antihuman κ LC antibody (Figure 1h). Although antihuman THP antibody stained the cytoplasm of epithelial cells in the loop of Henle (the production site of THP), the crystalline casts in the distal tubular lumens were not stained with the antibody (Figure 1i).

## Additional Investigations

After obtaining consent from the patient and the Research Ethics Committee of Akita University (approval number: 1830), characterization of the biochemical and structural properties of BJP-λ AK was performed. Urinary BJP-λ AK was purified in accordance with the procedures described in the Supplementary Methods. Urinary proteins in the fractions obtained at each purification step were analyzed by sodium dodecyl sulfate–polyacrylamide gel electrophoresis (Supplementary Figure S3), and the N-terminal amino acid sequence was determined using a protein sequencer (Supplementary Figure S4). The apparent molecular weight of BJP-λ AK was estimated to be approximately 55.3 kilodaltons in solution by size-exclusion chromatography coupled to multiangle light scattering analysis (Supplementary Figure S5), consistent with a dimer of BJP-λ AK. Sodium dodecyl sulfate–polyacrylamide gel electrophoresis analysis in reducing and nonreducing conditions indicated that BJP-λ AK dimers were covalently linked by disulfide linkage (Supplementary Figure S6).

Reverse transcription-polymerase chain reaction using total RNA from bone marrow cells was performed to obtain the full-length cDNA of BJP-λ AK, in accordance with the procedures described in the Supplementary Methods. The cloned cDNA had an open reading frame of 702 nucleotides (233 amino acids) encoding the full-length BJP-λ AK (Supplementary Figure S4). The analysis of the presence of signal peptides using the SignalP 5.0 peptide prediction server[S9] identified 2 potential cleavage sites between amino acids Gly16-Ser17 and Ser20-Tyr21. Based on the N-terminal amino acid sequencing of urinary BJP-λ AK, we determined the N-terminal 20 amino acid sequence as a signal peptide (Supplementary Figure S4).

As seen in the alignment of the deduced amino acid sequence of BJP-λ AK (Figure 2[S10]), the highly homologous germline $V_L$ and $J_L$ segments were IGLV3-21 members of the IGLV subgroup 3 (A)[5] (IGLV3S2,[S11] V2-14,[S12] and Humlv318[S13]) and IGLJ3,[5,S14] respectively. No mutations were detected in the CL region of BJP-λ AK.[S14] The sequence alignment revealed 7 amino acid mutations (T20A, G22E in the CDR1, E58D, T70A, Y85F, S92N in the CDR3, and D94N in the CDR3) compared with Humlv318 and 2 amino acid mutations (V96Q in the CDR3[S15] and L104V) compared with Jλ3.[5,S14]

Purified urinary BJP-λ AK was crystalized to obtain its X-ray crystal structure in accordance with the procedures described in the Supplementary Methods.[S16–S21] The structure of BJP-λ AK crystalized in the space group $P2_12_12_1$ was refined to a resolution of 1.77 Å with an $R_{work}$ of 22.8% and $R_{free}$ of 26.5% (Figure 3a; Supplementary Table S1). Electron density was traced well except for the CDR3 regions (W89–H95 in molecules A and B), the C-terminal region comprising residues E211–S213 in molecule A, and Gly66 in molecule B, which exhibited some disorder. As described previously for most other BJPs,[3] 2 monomers of BJP-λ AK possessing a Greek key Igβ-sandwich folds[S22] associated into a dimer in the asymmetric unit with the elbow angle between the $V_L$ and $C_L$ domains of molecule A at approximately 124° and that of molecule B at approximately 112°. The N-terminal region of BJP-λ AK (residues 1–13) contains a sheet switch motif including a β-bulge.[S23]

The interfaces of the crystallographic homodimer structure were analyzed using the Protein Interface, Surfaces, and Assemblies server,[S24] which showed that the interface interactions between the monomers were

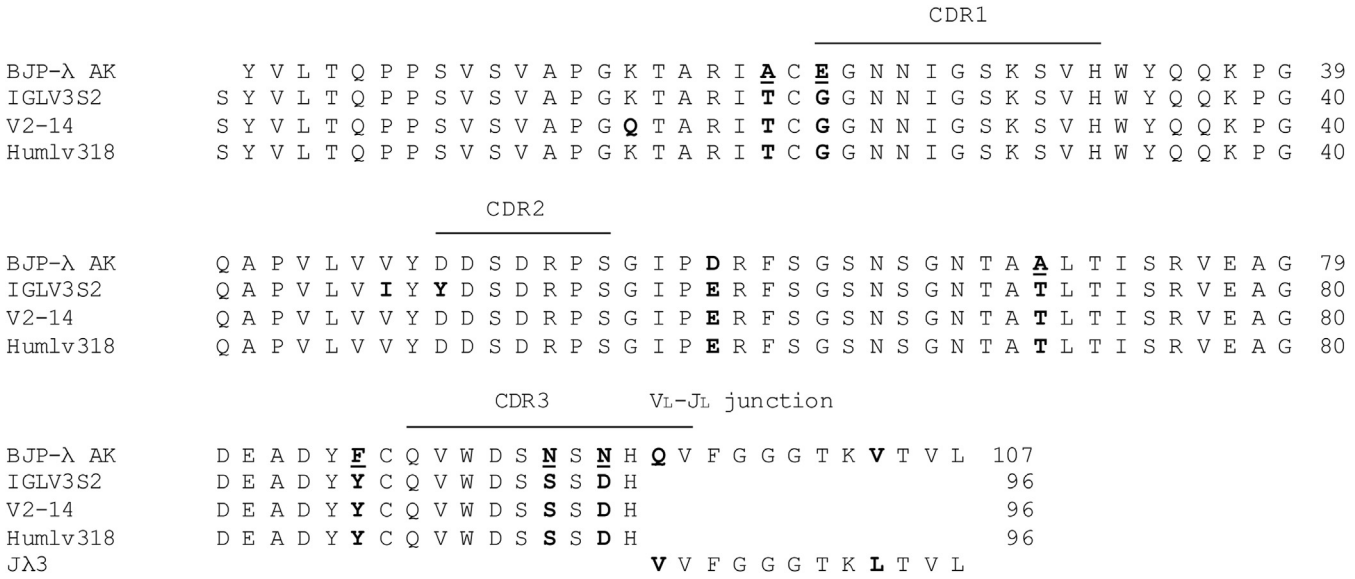


**Figure 2.** Primary structure of the variable ($V_L$) and joining ($J_L$) regions in BJP-λ AK aligned with highly homologous germline gene $V_L$ segments of IGLV subgroup 3 (A)[5] (IGLV3S2,[S11] V2-14,[S12] and Humlv318[S13]) and $J_L$ segment of IGLJ3 (Jλ3[5,S14]), using the Clustal Omega program.[S10] Mutated residues in IGLV subgroup 3 (A)[5] are indicated in bold and underlined when possibly indicating a significant physicochemical change. Different residues among IGLV subgroup 3 (A)[5] are also indicated in bold. CDR, complementarity-determining region.

specific and were not likely to be an artifact of crystal packing. Based on the Protein Interface, Surfaces, and Assemblies analysis, the $V_L/V_L$ and $C_L/C_L$ interfaces were predominately hydrophobic ($P = 0.13$) with 1613 Å$^2$ of buried solvent-accessible surface on average in each chain (Supplementary Figure S7). The somatic mutated residue Y85F was located in the hydrophobic interface. The somatic replacement of Tyr85 by phenylalanine may increase the hydrophobicity in the dimer interface. In addition, the dimer interface contained 15 hydrogen bonds with <3.6 Å distance (according to the criteria of Protein Interface, Surfaces, and Assemblies) between the monomers (Figures 3b and c). The amino acid residues Tyr34, Gln36, and Gln87 in the $V_L$ domains and Glu161, Thr162, Thr164, Ser166, Gln168, Ser169, Ser176, and Tyr178 in the $C_L$ domains of both monomers formed hydrogen bonds in the contact region.

In the BJP-λ AK crystal lattice, prominent packing interactions were mediated through hydrogen bond networks between the antiparallel β-sheets on the $C_L$ domain of neighboring symmetry molecules. Four hydrogen bonds between molecule A of dimer I and molecule B of dimer II were established. On the other site of dimer I, molecule B interacted with molecule A of dimer III through 7 hydrogen bonds (Supplementary Figures S8A–C). As shown in Supplementary Figures S8D–F, the packing was further stabilized by 3 salt bridges, including Glu22 (in molecule A of dimer I)–His189 (in molecule B of dimer IV), Arg75 (in molecule A of dimer I)–Glu81 (in molecule B of dimer V), and Asp49 (in molecule B of dimer I)–Lys190 (in molecule B of dimer VI). As described above, the mutation of G22E located in the CDR1 in molecule A of dimer I resulted in the formation of an additional salt bridge with His189 in molecule B of dimer IV. In other somatic mutations from the highly homologous germline, 4 hydrogen bonds were established with E58D (in molecule A of dimer I)–Tyr173 (in molecule B of dimer V), E58D (in molecule B of dimer I)–Gln185 (in molecule A of dimer VII), and S92N (located in the CDR3 in molecule B of dimer I)–Glu199 and –Gly200 (in molecule A of dimer V) in the crystal lattice.

## Diagnosis

The diagnosis of BJP-λ type MM-associated Ig λ LC crystalline cast nephropathy was made.

## Clinical Follow-Up

AK developed oliguria soon after admission and was treated with hemodialysis for 2 months. She also received chemotherapy for MM with a regimen of bortezomib, dexamethasone, lenalidomide, and pomalidomide. However, she died from her disease 6 months after the kidney biopsy specimen was obtained. An autopsy was not performed.

# DISCUSSION

Deposits of crystals cause kidney injury involving a broad variety of different pathophysiologic mechanisms. Mulay *et al.*[6] recently proposed a classification of crystalline nephropathies based on the localization of crystal deposits: vascular calcification or crystal embolism causing renal ischemia (type 1), intra- and

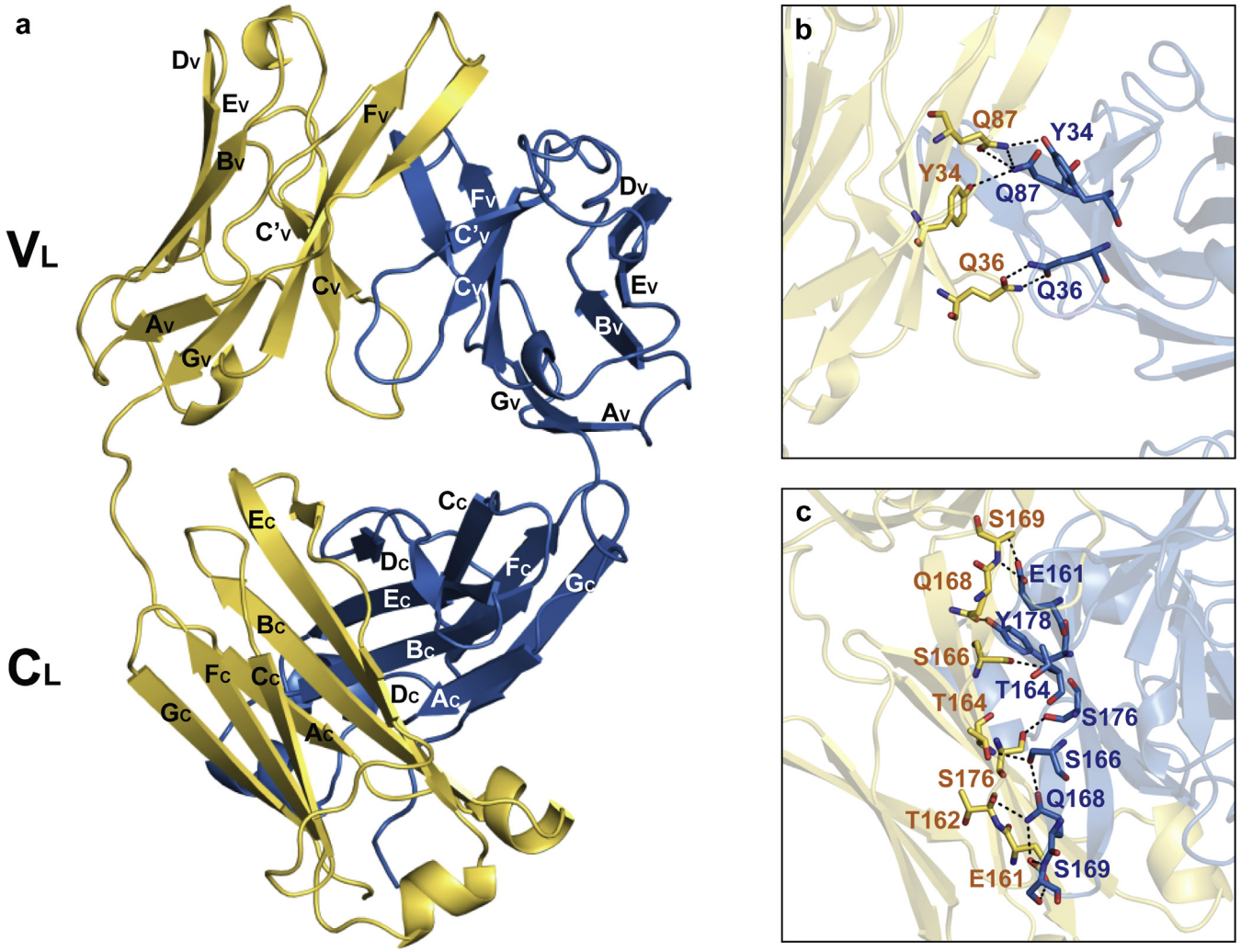


**Figure 3.** Crystal structure of Bence–Jones protein λ (BJP-λ AK). (a) The overall structure of a BJP-λ AK homodimer (Protein Data Bank code: 6L98). The 2 light chain molecules are colored in yellow (molecule A) and blue (molecule B). The β-strands that form the domains are marked with capital letters. Detailed views of the homodimer interface of (b) the $V_L$ domain and (c) the $C_L$ domain stabilized by hydrogen bonds. Hydrogen bonds are shown as black dashed lines. $C_L$, light chain constant domain; $V_L$, light chain variable domain.

extratubular crystalline precipitates causing tubular injury (type 2), and nephrolithiasis causing obstructive nephropathy (type 3). In type 2 crystalline nephropathies, acute/chronic supersaturation of metabolites, minerals, or proteins such as monoclonal Ig LCs, cryoglobulin, and myoglobin can promote crystal formation, leading to an acute/chronic episode of crystal-induced tubular cell injury, interstitial inflammation, and impairment of renal function.[6] Monoclonal Ig LC crystals are rarely deposited in the proximal tubular epithelial cells, causing proximal tubulopathy with or without Fanconi syndrome, and in the tubular lumens, causing cast nephropathy.[6,7] Monoclonal Ig LC crystals also precipitate in intrarenal phagocytes, causing crystal-storing histiocytosis.[6]

Table 1 summarizes the clinicopathologic findings in 9 cases of MM-associated Ig LC crystalline cast nephropathy reported since 2000[S1–S8] and in our case. The mean age of the patients was 63 years (range, 48–73 years), and all patients presented with AKI. Although various types of monoclonal Igs were detected, it was notable that 3 patients had IgD-λ type proteins: in Nasr's cohort of ordinary myeloma cast nephropathy,[4] only 6% of patients had IgD type monoclonal Igs. There was a clear dominance of λ-type LC confirmed by positive λ LC staining of crystals in 6 patients. Moreover, according to the review of 9 cases of MM-associated Ig LC crystalline cast nephropathy reported before 2000 by Kanno *et al.*,[S1] λ-type LCs were also commonly found in the tubular lumen as opposed to ordinary myeloma cast nephropathy,[4] in which κ-type LCs are generally responsible for renal disorders. In general, the crystalline casts were positively stained with trichrome and eosin, but not with periodic acid–Schiff, as in our case. Accumulation of crystalline casts was observed both in the proximal and distal tubular

**Table 1.** Multiple myeloma–associated Ig light chain crystalline cast nephropathy (summary of reported cases since 2000)

| Reference, year | Age/sex | Clinical category | MIg | BJP | Dyeability of crystals | Distribution of crystals | HD | Treatment for MM | Outcome | cDNA cloning homologous $V_L$ gene |
|---|---|---|---|---|---|---|---|---|---|---|
| S1, 2001 | 71/M | AKI | IgD-λ | + | E (+)<br>IgD (ND) λ (–) κ (–) | Tubular lumen, Bowman's space, BM | + | ND | Died (50 d after admission) | |
| S2, 2005 | 73/F | AKI | ND | + | MT (+) E (+)<br>λ (+) κ (–) | Tubular lumen, glomerulus, BM | + | MET, ADM, VCR, CPM | Died (10 mo after diagnosis) | |
| S3, 2011 | 58/M | AKI | IgD-λ | AN | MT (+) E (+)<br>IgD (–) λ (+) | Tubular lumen, Bowman's space, BM | + | BOR, DEX | Died (30 mo after diagnosis) | IGLV1-51 |
| S4, 2014 | 57/M | AKI | IgG-λ | + | E (+) THP (–)<br>IgG (ND) λ (+) κ (–) | Tubular lumen | + | BOR, DEX | Improved, being evaluated for ASCT | |
| S5, 2014 | 48/M | AKI | IgA-λ | + | ND | Tubular lumen, tubular epithelial cytoplasm | | BOR, LEN, DEX, CPM | Slowly improved | |
| S5, 2014 | 56/M | AKI | IgG-κ | + | E (+) | Tubular lumen, tubular epithelial cytoplasm | | BOR, DEX LEN | Refractory to chemotherapy | |
| S6, 2016 | 72/F | AKI | IgD-λ | + | EM (+) PAS (–)<br>IgD (ND) λ (+) κ (–) | Proximal tubular lumen | | BOR, DEX | CR with normal renal function (for 2 yr) | |
| S7, 2016 | 59/F | AKI | IgA-λ | ND | E (+) T (+) PAS (–)<br>IgA (ND) λ (+) κ (–) | Distal tubular lumen | | BOR, DEX LEN | Died (16 d after biopsy) | |
| S8, 2020 | 66/F | AKI | BJP-κ | + | E (+) PAS (–)<br>THP (+) λ (–) κ (+) | Distal tubular lumen<br>Proximal tubular cells | | BOR, CPM DEX, LEN | Lost to follow-up | |
| Present case, 2020 | 73/F | AKI | BJP-λ | + | MT (+) E (+) PAS (–)<br>THP (–) λ (+) κ (–) | Distal tubular lumen | + | BOR, DEX<br>LEN, POM | Died (6 mo after diagnosis) | IGLV3-21 (IGLV3S2, V2-14, Humlv318)[5] |

ADM, adriamycin; AKI, acute kidney injury; AN, anuria; ASCT, autologous stem cell transplant; BJP, Bence–Jones protein; BM, bone marrow; BOR, bortezomib; CPM, cyclophosphamide; CR, complete remission; DEX, dexamethasone; E, eosin; EM, elastica-Masson; HD, hemodialysis; LC, light chain; LEN, lenalidomide; MET, methasone; MIg, monoclonal Ig; MM, multiple myeloma; MT, Masson's trichrome; ND, not detailed; PAS, periodic acid–Schiff; POM, pomalidomide; T, trichrome; THP, Tamm–Horsfall glycoprotein; VCR, vincristine; $V_L$, light chain variable domain.

lumens, as well as in the bone marrow in 3 cases. A large portion of the cases were reported to have rapidly progressive course with a poor prognosis. On the other hand, complete remission with normal renal function for 2 years was achieved using bortezomib-dexamethasone therapy in 1 case.[S6] In this case, serum creatinine level was 1.90 mg/dl at the time the biopsy specimen was obtained. Therefore, early diagnosis and bortezomib-based chemotherapy may improve the prognosis of MM-associated Ig LC crystalline cast nephropathy. The safety and efficacy of bortezomib-based therapies in MM patients with renal impairment has been established.[8]

cDNA cloning was performed only in 2 cases, including our case. In the case of Toly-Ndour *et al.*,[S3] the most homologous germline gene $V_L$ and $J_L$ segments were IGLV1-51[5] and J3,[5] respectively. They suggested that 6 of the 11 observed mutations in the $V_L$ region might contribute to pathologic properties. In our case, the most homologous germline gene $V_L$ and $J_L$ segments of BJP-λ AK were Humlv318[S13] and J3,[5,S14] respectively. There were 9 mutations in the $V_L$ and $J_L$ segments of BJP-λ AK. Among them, 4 amino acids were present in the CDR1 or CDR3 region: G22E, D94N, and V96Q can modify the surface charge and hydrophobicity, respectively. In addition, T20A and Y85F can also affect the hydrophobicity surrounding the CDR1 or CDR3 region.

In ordinary myeloma cast nephropathy, cast formation occurs in the distal tubular lumens through reciprocal binding with THP.[1,2,7] THP contains the Ig FLC-binding domain (CAHWSGHC): the cysteines at the N- and C-termini of the domain are linked via an intramolecular disulfide bridge.[2,9] This bridge places the 2 histidines in close proximity to permit potential ionic interaction with the CDR3 domain in BJPs.[2,9] Ying *et al.*[9] reported that the secondary structure and key amino acid residues in the CDR3 of Ig FLCs are critically important determinants of the molecular interaction with THP. In our case, the accumulation of crystalline casts was observed in the distal tubular lumens; however, THP was not stained within the casts on immunohistochemical studies. This suggests that the CDR3 domain of BJP-λ AK has a low binding affinity toward THP, and thus crystallization occurs without reciprocal binding with THP. On the contrary, in the case reported by Lerner *et al.*,[S8] crystalline casts within the distal tubular lumens colocalized with THP.

Cast formation propensity in cases of MM-associated Ig LC crystalline cast nephropathy may depend on structural characteristics of the disease-causing BJP, in addition to the tubular luminal environment (i.e., pH, ionic composition, concentration, and flow rate of tubular fluid).[7] We present the first report of the 3-dimensional structure of BJP that induced MM-associated Ig LC crystalline cast nephropathy using

X-ray crystallography (Figure 3; Supplementary Figures S7 and S8). BJP-λ AK assembled into a homodimer through hydrophobic and hydrogen bond interactions between LC monomers. Previous biophysical findings indicated that low fold stability and high protein dynamics of BJP correlated with LC amyloidogenicity.[3,S25] The hydrophobic and hydrogen bond interaction between LC monomers promoted thermal stability and thereby interfered with fibrillogenesis of BJP-λ AK. In addition, as in other β-sheet–rich proteins, the $V_L$ domain of BJP-λ AK contains structural features to avoid undesired protein aggregation and formation of amyloid fibril.[S23,S26] The sheet switch motif including a β-bulge in the N-terminal region of LCs is proposed to act as an antiaggregation domain for β-strands B and G. The N-terminal region of BJP-λ AK contains the sheet switch motif with 2 conserved proline residues at positions 6 and 7 that are important to stabilize the sheet switch.[S27]

Previous studies with mutation of Pro40 (Pro38 in BJP-λ AK) in the residue 40–44 $C_V$-$C'_V$ loop (residues 38–42 in BJP-λ AK) that forms part of the homodimer interface also proposed that the $C_V$-$C'_V$ loop and Pro40 may play a key role in the stability of the overall quaternary structure.[S28,S29] Replacement of Pro40 with a hydrophobic residue Leu caused structural destabilization of the $C_V$-$C'_V$ loop, which is presumed to be involved in the initial conformational change leading to amyloid formation. Residues 38–42 in the $C_V$-$C'_V$ loop, including Pro38 of BJP-λ AK, are highly conserved among IGLV3-21 members, which is thought to play a key role in the stabilization of residues 40–46 in framework region 2 segment (residues 38–44 in BJP-λ AK), and the positioning of Gln36 in the β-strand $C_V$ for a hydrogen bond interaction across the homodimer interface. Furthermore, crystal packing analysis (Supplementary Figure S8) showed that somatic mutated residues contribute to crystal formation through formation of a salt bridge and hydrogen bonds between symmetry-related dimers. G22E and S92N are likely to be more influential mutations for the crystal packing interaction. Substitution with a negatively charged longer side chain at G22E mutation may induce more intimate intermolecular interactions through formation of a novel salt bridge with the His189 of symmetry-related dimer. In addition, the S92N mutation formed 2 novel hydrogen bonds between symmetry-related dimers: S92N ND2–E199 OE1 of symmetry-related dimer and S92N OD1–G200 N of symmetry-related dimer. As reported previously,[S30] mutations of molecular surface residues such as G22E and S92N may be related to intermolecular interactions for crystal packing and promoting protein crystallization.

**Table 2.** Teaching points

| |
|---|
| 1. MM-associated Ig LC crystalline cast nephropathy was classified into tubular crystalline nephropathy (type 2) in the recent classification of crystalline nephropathies. |
| 2. This nephropathy is a rare but distinct variant form of myeloma cast nephropathy. |
| 3. Clinicopathologic characteristics of this nephropathy are rapid progression and poor outcomes, λ LC dominance, crystalline cast formation both in the proximal and distal tubular lumens, and with or without incorporation of THP in distal tubular casts. |
| 4. Early diagnosis and chemotherapy for MM in the new era can improve the prognosis of this nephropathy. |
| 5. Cast formation in this nephropathy may depend on structural characteristics of the disease-causing BJP. |

BJP, Bence–Jones protein; LC, light chain; MM, multiple myeloma; THP, Tamm–Horsfall glycoprotein.

## CONCLUSION

In conclusion, we show the primary and 3-dimensional structures of the disease-causing BJP-λ in a patient with MM-associated Ig λ LC crystalline cast nephropathy. Further accumulation of structural characterization data of the disease-causing BJP will be necessary to elucidate the mechanism of crystalline cast formation. Teaching points are shown in Table 2.

## DISCLOSURE

NT has received grants and personal fees from Novartis Pharmaceuticals, Pfizer, and Otsuka Pharmaceutical; personal fees from Bristol Myers Squibb; and grants from Kyowa Hakko Kirin, Astellas Pharma, Chugai Pharmaceutical, Asahi Kasei Pharma, Ono Pharmaceutical, and Eisai Pharmaceuticals; outside of the submitted work. All the other authors declared no competing interests.

## ACKNOWLEDGEMENTS

Structural studies in this report were supported in part by Japan Society for the Promotion of Science Grant-in-Aid for Scientific Research Grants 19K17728 (to MN) and 19K07011 (to HM), and private donations from Ken Satoh, Satoh Naika Clinic, Sakata, Japan, and Masaru Togashi, Akita Renal, Collagen and Rheumatic Disease Clinic, Akita, Japan.

## SUPPLEMENTARY MATERIAL

Supplementary File (Word)

**Supplementary Methods.**

**Table S1.** X-ray data collection and refinement statistics.

**Figure S1.** Bone marrow findings. May–Giemsa stain (original magnification ×200).

**Figure S2.** Kidney biopsy findings.

**Figure S3.** Purification of BJP-λ AK from the patient's urine.

**Figure S4.** cDNA and deduced amino acid sequences of BJP-λ AK (GenBank accession number LC508016).

**Figure S5.** Plot of the apparent molecular weight of the purified BJP-λ AK versus elution volume in size-exclusion chromatography coupled to multiangle light scattering.
**Figure S6.** Disulfide-linked dimer formation of BJP-λ AK.
**Figure S7.** Dimerization of BJP-λ AK.
**Figure S8.** Crystal packing of BJP-λ AK.
**Supplementary References.**

## REFERENCES


1. Sethi S, Rajkumar SV, D'Agati VD. The complexity and heterogeneity of monoclonal immunoglobulin-associated renal diseases. *J Am Soc Nephrol*. 2018;29:1810–1823.
2. Sanders PW. Mechanisms of light chain injury along the tubular nephron. *J Am Soc Nephrol*. 2012;23:1777–1781.
3. Blancas-Mejia LM, Misra P, Dick CJ, et al. Immunoglobulin light chain aggregation. *Chem Commun (Camb)*. 2018;54:10664–10674.
4. Nasr SH, Valeri AM, Sethi S, et al. Clinicopathologic correlations in multiple myeloma: a case series of 190 patients with kidney biopsies. *Am J Kidney Dis*. 2012;59:786–794.
5. Pallarès N, Frippiat JP, Giudicelli V, et al. The human immunoglobulin lambda variable (IGLV) genes and joining (IGLJ) segments. *Exp Clin Immunogenet*. 1998;15:8–18.
6. Mulay SR, Shi C, Ma X, et al. Novel insights into crystal-induced kidney injury. *Kidney Dis (Basel)*. 2018;4:49–57.
7. Doshi M, Lahoti A, Danesh FR, et al. Paraprotein-related kidney disease: kidney injury from paraproteins–What determines the site of injury? *Clin J Am Soc Nephrol*. 2016;11:2288–2294.
8. Terpos E, Kleber M, Engelhardt M, et al. European Myeloma Network guidelines for the management of multiple myeloma-related complications. *Haematologica*. 2015;100:1254–1266.
9. Ying WZ, Allen CE, Curtis LM, et al. Mechanism and prevention of acute kidney injury from cast nephropathy in a rodent model. *J Clin Invest*. 2012;122:1777–1785.